Available online at www.sciencedirect.com
ScienceDirect
Trans. Nonferrous Met. Soc. China 26(2016) 849−858
Transactions of Nonferrous Metals Society of China
www.tnmsc.cn

Formation mechanism and crystal simulation of Na_2O-doped calcium aluminate compounds

Yong-pan TIAN, Xiao-lin PAN, Hai-yan YU, Gan-feng TU

School of Metallurgy, Northeastern University, Shenyang 110819, China

Received 23 April 2015; accepted 10 November 2015

Abstract: Calcium aluminate clinkers doped with Na_2O were synthesized using analytically pure reagents $CaCO_3$, Al_2O_3, SiO_2 and Na_2CO_3. The effects of Na_2O-doping on the formation mechanism of calcium aluminate compounds and the crystal property of $12CaO\cdot7Al_2O_3$ ($C_{12}A_7$) cell were studied. The results show that the minerals containing Na_2O mainly include $2Na_2O\cdot3CaO\cdot5Al_2O_3$ and $Na_2O\cdot Al_2O_3$, when the Na_2O content in clinkers is less than 4.26% (mass fraction). The rest of Na_2O is mainly doped in $12CaO\cdot7Al_2O_3$, which results in the decrease of the crystallinity of $12CaO\cdot7Al_2O_3$. The crystallinity of $2Na_2O\cdot3CaO\cdot5Al_2O_3$ is also inversely proportional to the Na_2O content in clinkers. The formation processes of $2Na_2O\cdot3CaO\cdot5Al_2O_3$ and $12CaO\cdot7Al_2O_3$ can be divided into two ways, which are the direct reactions of raw materials and the transformation of $CaO\cdot Al_2O_3$, respectively. The simulation shows that the covalency of O—Na bond in Na_2O-doped $12CaO\cdot7Al_2O_3$ cell is weaker than those of O—Ca and O—Al bonds. The free energy of the unit cell increases because of Na_2O doping, which results in the improvement of chemical activity of $12CaO\cdot7Al_2O_3$. The leaching efficiency of Al_2O_3 in clinker is improved from 34.81% to 88.17% when the Na_2O content in clinkers increases from 0 to 4.26%.

Key words: calcium aluminate; Na_2O-doping; formation mechanism; crystal structure; sintering; computer simulation

1 Introduction

The low-grade bauxites and non-bauxite sources such as nepheline, clay and fly ash are widely distributed in China. It is suitable to extract alumina from these sources by the lime sintering process since dry materials can be used during the sintering process, reducing the energy consumption of the alumina production industry. However, the application of the lime sintering process is restricted by the defects including the high consumption of calcium, large amount of slag and poor leaching property of clinkers. The clinker of the lime sintering process mainly consists of $12CaO\cdot7Al_2O_3$ ($Ca_{12}Al_{14}O_{33}$, $C_{12}A_7$), $2CaO\cdot SiO_2$ (C_2S), $CaO\cdot Al_2O_3$ ($CaAl_2O_4$, CA) and $2CaO\cdot Al_2O_3\cdot SiO_2$ (C_2AS). The calcium aluminate compounds, which can decompose in the sodium carbonate solution, are mainly $C_{12}A_7$ and CA. The previous researches [1,2] showed that the doping of Na_2O in the sintering process could improve the leaching performance of clinkers and reduce the consumption of CaO. Moreover, the results showed that the lattice constants of $C_{12}A_7$ increase with the increase of the molar ratio of Na_2O to Al_2O_3 (N/A ratio) of clinker. However, the details of phase structures were not analyzed, and the mechanisms by which Na_2O affects the calcium aluminate compounds were unknown.

In the Na_2O-doped $CaO-Al_2O_3$ system, the amounts of $C_{12}A_7$ and $2Na_2O\cdot3CaO\cdot5Al_2O_3$ ($Na_4Ca_3(AlO_2)_{10}$) reach the maximum as the sodium content in CA increases to 10% (mass fraction) [3]. Additionally, the crystallinity of $C_{12}A_7$ decreased with the doping of Na_2O while that of CA increased [4]. FUKUDA et al [5] reported that Al^{3+} ions were substituted by Si^{4+} ions and Ca^{2+} ions were substituted by Na^+ ions, when $3CaO\cdot Al_2O_6$ (C_3A) was doped with Na^+ and Si^{4+} ions. Many reports [6−11] showed that the properties of crystal structures could be analyzed by the Material Studio. BRIK et al [12] showed that the structural and electronic properties of the two Cr^{3+}-bearing systems ($NaCrSi_2O_6$ and $LiCrSi_2O_6$) could be studied by the CASTEP module of Materials Studio package with two *ab* initio DFT-based calculations. WU et al [13] observed that the coordination number of Al atom as well as its

Foundation item: Projects (51174054, 51104041, 51374065) supported by the National Natural Science Foundation of China; Project (N130402010) supported by the Fundamental Research Funds for the Central Universities of China
Corresponding author: Xiao-lin PAN; Tel: +86-24-83686460; E-mail: panxl@smm.neu.edu.cn
DOI: 10.1016/S1003-6326(16)64176-6

amphoteric property in the melt of xCaO·(1−x)Al_2O_3 (x represents mole fraction) and the microstructure properties of xCaO·(1−x)Al_2O_3 could be studied by the molecular dynamics simulation using Materials Studio. PAN et al [14] reported that the free energy of the $C_{12}A_7$ cell calculated by the Materials Studio increased because of the absence of some Ca atoms in $C_{12}A_7$ cells. In this work, the compounds containing Na_2O, the doping mechanism of Na_2O in compounds and the chemical activity of the $C_{12}A_7$ crystal structure with or without Na_2O doping as well as leaching characteristics of clinkers were investigated. Meanwhile, the phase constitutions, the distribution characteristics of phases in micro-regions and the crystal structure of $C_{12}A_7$ doped with Na_2O were also investigated through Material Studio.

2 Experimental

2.1 Materials

Analytically pure reagents ($CaCO_3$, Al_2O_3, SiO_2 and Na_2CO_3) were used in the current work. In Na_2O-doped CaO−Al_2O_3−SiO_2 system, the mass ratio of Al_2O_3 to SiO_2 (A/S) was about 1.6 and the molar ratio of CaO to Al_2O_3 (C/A) was about 0.85. The C/A ratios of Na_2O-doped CaO−Al_2O_3 system were 0.6 and 1.0. The amounts of Na_2O in clinker were represented by the values of the molar ratios of Na_2O to Al_2O_3 (N/A). The mixed materials were sintered at 1200 ℃ or 1350 ℃ in a $MoSi_2$ resistance furnace (KSL−1700−A2). Then, the clinkers were ground to 100 μm.

2.2 Methods

The X-ray diffraction (XRD) data were collected on a Philips PW3040/60 with Cu K_α (λ=1.54056 Å) radiation operated at 40 kV and 40 mA. The K_α ray included two kinds of wavelength, which were $K_{\alpha1}$ and $K_{\alpha2}$, respectively. The data were analyzed by the MDI Jade with the database PDF2−2004. The cubic spline method was used to subtract the background and the peaks generated by the $K_{\alpha2}$ radiation were also subtracted as the ratio of $K_{\alpha1}/K_{\alpha2}$ was 2.0. The Pseudo−Voigt function was used during the fitting processes of spectra, and nearly 100 peaks were fitted for every spectrum. The microstructural analyses were carried out by scanning electron microscopy (SEM, SHIMADZU SSX−550) and energy-dispersive X-ray spectroscopy (EDS, DX−4). The samples were polished flat in water-free ethylene glycol using SiC papers, cleaned by ultra-sound in water-free ethylene glycol and coated with gold by sputtering.

The Visualizer module of Materials Studio was used to establish three-dimensional models of $C_{12}A_7$ cells with or without Na_2O doping, which provided the foundation models for the subsequent calculation. The lattice parameter, the unit cell volume and free energy of the crystal structure, as well as the population and length of chemical bond were analyzed through the geometry optimization of the crystals. The CASTEP module of Materials Studio was used during the optimization process. The generalized gradient approximation (GGA) and the corresponding exchange-correlation potential (PBE) were used during the geometry optimization of the crystals through the BFGS algorithm while the Ultrasoft was selected as pseudopotential. The energy cut-off value was 340.0 eV. The SCF tolerance was 1.0×10^{-6} eV/atom. The results were obtained after large numbers of iterations. The original crystallographic data of the calculation were taken from the inorganic crystal structure database (ICSD).

2.3 Leaching conditions

The leaching experiments were carried out in a thermostatic water bath. The sintered clinkers were leached by the sodium carbonate and sodium hydroxide solution at 80 ℃ for 30 min. The liquid-to-solid ratio for leaching was 10. The sodium carbonate concentration of the solution was 80 g/L (in the form of Na_2O) and the sodium hydroxide concentration of the solution was 15 g/L (in the form of Na_2O). The leaching residues were washed to neutrality with hot water and dried under 90 ℃. The chemical compositions of clinkers and residues were analyzed by X-ray fluorescence (XRF−1800). The alumina leaching efficiencies (η_{AO}) of Na_2O-doped CaO−Al_2O_3−SiO_2 system clinker and Na_2O-doped CaO−Al_2O_3 system clinker were calculated according to Eq. (1):

$$\eta_{AO}=\left(1-\frac{(A/C)_{residue}}{(A/C)_{clinker}}\right)\times100\% \quad (1)$$

where $(A/C)_{residue}$ and $(A/C)_{clinker}$ are the mass ratios of Al_2O_3 to CaO of leached residues and sintered clinkers, respectively.

3 Results and discussion

3.1 Phase species and formation mechanism

As shown in Fig. 1(a), pure $Na_4Ca_3(AlO_2)_{10}$ was synthesized after sintering at 1200 ℃ for 30 min. There is no $Na_4Ca_3(AlO_2)_{10}$ card in the PDF2−2004. But the XRD pattern of $Na_4Ca_3(AlO_2)_{10}$ is similar to that in Ref. [3]. CA was synthesized after sintering at 1600 ℃ for 60 min. CA and Na_2CO_3 were sintered at 1350 ℃ for 60 min when the N/A ratio is 0.33. The XRD patterns of clinkers are shown in Fig. 1(b). Most of CA transforms to $C_{12}A_7$ and $Na_4Ca_3(AlO_2)_{10}$. Some $Na_2O\cdot Al_2O_3$ (NA) also exists in clinkers.

The compositions of Na_2O-doped CaO−Al_2O_3−SiO_2

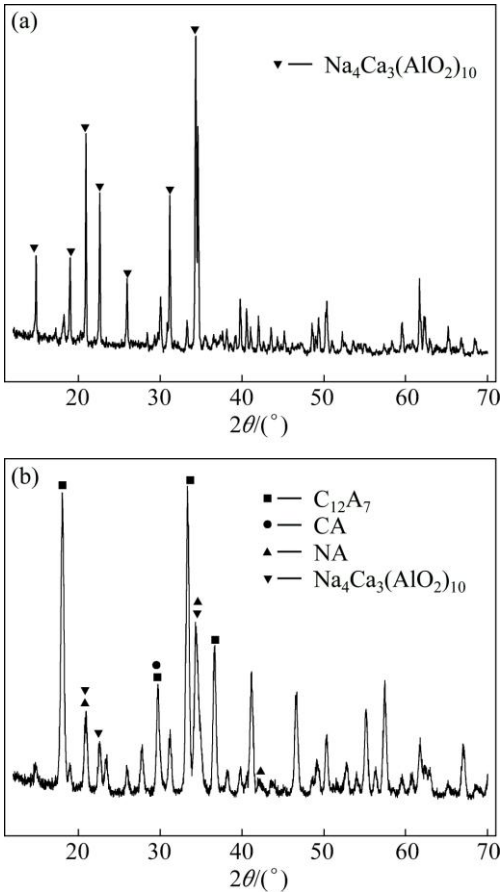

Fig. 1 XRD patterns of Na_2O−CaO−Al_2O_3 system clinkers: (a) $Na_4Ca(AlO_2)_{10}$; (b) Clinker

system clinkers are shown in Table 1. The phases of clinkers with different N/A ratios are shown in Fig. 2. The phases containing Al_2O_3 consist of $C_{12}A_7$, CA, NA, CaO·$2Al_2O_3$ (CA_2), $Na_4Ca_3(AlO_2)_{10}$ and C_2AS. The phases containing SiO_2 consist of C_2AS, β-C_2S and γ-C_2S. The phases containing Na_2O consist of $Na_4Ca_3(AlO_2)_{10}$ and NA. In addition, trace amounts of $Ca_{8.5}NaAl_6O_{18}$ and $Ca_{8.25}Na_{1.5}Al_6O_{18}$ are also found. When the N/A ratio is less than 0.04, small amount of CA_2 and some un-reacted CaO and Al_2O_3 exist in clinkers. As the N/A ratio increases to 0.17, CaO and Al_2O_3 react completely. The amount of CA_2 is also inversely proportional to the amount of Na_2O in clinkers. No CA_2 exists in clinkers as the N/A ratio increases to 0.17, which indicates that Na_2CO_3 accelerates the transformation reactions of CA_2. The melting temperature of Na_2CO_3 is about 850 ℃ and the decomposition temperature is about 1750 ℃, so Na_2CO_3 melts at the clinkering temperature of 1350 ℃. The diffusion speeds of ions are accelerated by the melting of Na_2CO_3, which results in higher reaction velocities of CaO, Al_2O_3 and CA_2. The sintering temperature is higher than the formation temperature of $Na_4Ca_3(AlO_2)_{10}$. So, some $Na_4Ca_3(AlO_2)_{10}$ form before the sintering temperature reaches 1350 ℃ in the Na_2O-doped CaO−Al_2O_3−SiO_2 system clinkers. The formation processes of $Na_4Ca_3(AlO_2)_{10}$ and $C_{12}A_7$ can be divided into two ways, which are the transformation of CA (Eq. (2) [3]) and the direct reaction among Na_2CO_3, CaO and Al_2O_3, respectively.

$$39(CaO\cdot Al_2O_3)+10Na_2CO_3=2(12CaO\cdot 7Al_2O_3)+5(2Na_2O\cdot 3CaO\cdot 5Al_2O_3)+10CO_2\uparrow \quad (2)$$

Table 1 Chemical compositions of Na_2O-doped clinkers (mass fraction, %)

N/A	Na_2O	Al_2O_3	SiO_2	CaO
0.00	0.00	30.62	19.15	50.24
0.04	0.81	30.20	19.00	49.98
0.17	2.97	28.57	19.26	49.19
0.24	4.26	29.44	18.25	48.05

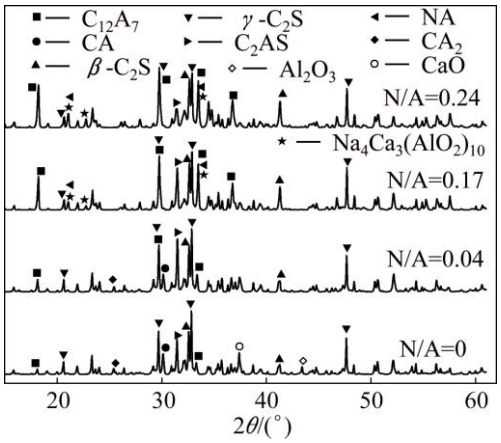

Fig. 2 XRD patterns of clinkers with different N/A ratios

The intensities of characteristic peaks of different phases are shown in Table 2. With the doping of Na_2O and the absolute reaction of CaO and Al_2O_3, the intensity of the characteristic peak of C_2AS at 2θ value of 31.47° increases firstly and then decreases as the N/A ratio increases from 0.04 to 0.24. The increase of the amount of C_2AS may be due to the higher reaction velocities of CaO, Al_2O_3 and SiO_2 accelerated by the melting of Na_2CO_3, and the decrease may be due to the lower forming velocity of C_2AS compared with other compounds. C_2S exists as the form of β-C_2S when the temperature is above 800 ℃ and then transforms to γ-C_2S with the decrease of temperature. The Na_2O-doped clinkers contain large amounts of β-C_2S, which indicates that Na_2O restrains the transformation of β-C_2S. Moreover, the decrease of the intensity of the characteristic peak of γ-C_2S also suggests the reducing of γ-C_2S content. The intensities of the characteristic peaks at 2θ values of 18.23° and 21.10° increase as the N/A ratio increases from 0 to 0.24. The results suggest the increase of the $C_{12}A_7$ and $Na_4Ca_3(AlO_2)_{10}$ contents. On

Table 2 Intensities of peaks of phases in Na_2O-doped $CaO-Al_2O_3-SiO_2$ system clinkers

N/A	C_2AS (2θ=31.47°)	γ-C_2S (2θ=47.65°)	CA (2θ=30.12°)	$C_{12}A_7$ (2θ=18.23°)	$Na_4Ca_3(AlO_2)_{10}$ (2θ=21.10°)	$Na_4Ca_3(AlO_2)_{10}$ and $C_{12}A_7$(2θ=33.33°)
0	18793	22360	11073	2578	−	6069
0.04	26078	20354	8323	5957	869	8556
0.17	17714	20957	−	14726	3688	21817
0.24	7131	16020	−	15468	5319	16862

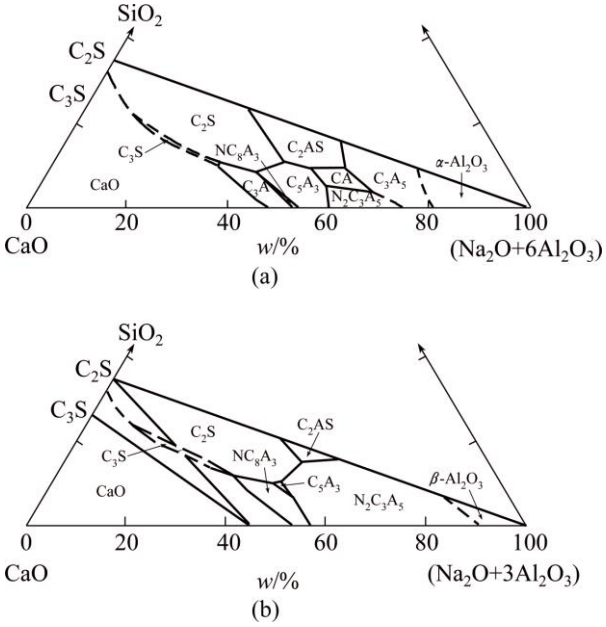

Fig. 3 $Na_2O-CaO-Al_2O_3-SiO_2$ quarternary system phase diagram [15]: (a) N/A=0.17; (b) N/A=0.33

the contrary, the content of CA decreases with the increase of Na_2O content in clinkers. CA disappears as the N/A ratio increases to 0.17. Moreover, the results are in accordance with the phase diagram, which suggests that the zone of C_2AS gradually decreases while the zone of $Na_4Ca_3(AlO_2)_{10}$ increases with the N/A ratio increasing from 0.17 (Fig. 3(a)) to 0.33 (Fig. 3(b) [15]). No CA exists in the system when the N/A ratio is equal to 0.33.

The characteristic peak at 2θ value of 33.33° is the peak of $C_{12}A_7$ when the N/A ratio is 0 and then becomes a mixed peak of $C_{12}A_7$, $Na_4Ca_3(AlO_2)_{10}$ and NA when the clinkers are doped with Na_2O. Small amount of NA exists in the clinkers, so the contribution of CA to the intensity of the mixed peak can be ignored. The crystal faces of $C_{12}A_7$ represented by the characteristic peaks at 2θ values of 18.23° and 33.33° are (211) and (420), respectively. The intensity of the characteristic peak of $C_{12}A_7$ at 2θ value of 33.33° is stronger than that of the characteristic peak of $C_{12}A_7$ at 2θ value of 18.23° when the N/A ratio is 0. The intensity of the characteristic peak at 2θ value of 33.33° decreases from 21817 to 16862, while the intensity of the characteristic peak at 2θ value of 18.23° increases from 14726 to 15468 when the N/A ratio increases from 0.17 to 0.24. The results suggest that the $C_{12}A_7$ formed by the transformation of CA prefers to growing in the crystal face (211).

3.2 Microstructures of clinkers

As shown in Fig. 4, the representative microstructure of the clinker, when the N/A ratio is 0.04, displays three gray scales: the dark gray, the medium gray, and the light gray. The compositions of the micro-regions of Points *A*, *B* and *C* are listed in Table 3. The molar ratio of CaO to SiO_2 in the micro-region of Point *A* is close to 2, indicating that the light gray regions stand for C_2S. The molar ratio of CaO to Al_2O_3 at

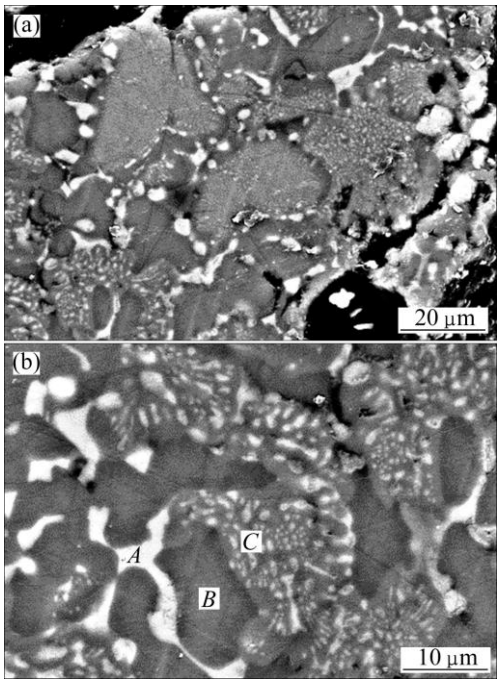

Fig. 4 BSE images of sintered clinkers at N/A ratio of 0.04 and C/A ratio of 0.88: (a) Lower magnification; (b) Higher magnification

Table 3 Mole fractions of elements in clinkers determined by EDS (%)

Point	Na	Al	Si	Ca	O
A	0.75	3.53	14.30	27.44	53.99
B	3.59	26.92	0.22	19.67	49.60
C	0.26	19.04	6.45	21.08	53.17

Point *B* is close to 1.71. So, the dark area is the distribution area of $C_{12}A_7$. The Na_2O content in $C_{12}A_7$ is 4.33% (mass fraction). The chemical formula can be written as $0.93Na_2O \cdot 10CaO \cdot 7Al_2O_3$. At Point *C* where CaO is divided into two parts, the molar ratios of CaO to Al_2O_3 and CaO to SiO_2 are close to 1 and 2, respectively. Therefore, the region of Point *C* consists of CA and C_2S and the medium gray region stands for CA. Na_2O is mainly doped in $C_{12}A_7$ since the Na_2O content in the region of $C_{12}A_7$ is the highest. The analysis results of Ca and O elements in different areas do not show significant differences as the Na, Al and Si elements do.

Map scanning results are shown in Fig. 5. The high light areas in Figs. 5(b)−(f) are the main distribution areas of Na, Al, Si, Ca and O elements, respectively. The high light area of the picture is the main distribution area of the element. As shown in Fig. 5(b), it is obvious that Na_2O mainly exists in the dark gray area, which is the distribution area of $C_{12}A_7$. Figure 5(d) shows the scopes of C_2S and $C_{12}A_7$ clearly. According to Figs. 5(e) and (f), the distributions of O and Ca do not show significant differences, which is consistent with the analysis results of EDS.

BSE images of clinkers at N/A ratio of 0.24 are shown in Fig. 6. The analysis results of EDS are given in Table 4. It can be clearly seen that the phases distribute in different regions by mole fraction of elements. The lightest area is the distribution area of C_2S. It can be calculated that the Na_2O content doped in C_2S is about 1.97%. The regions represented by Points *E* and *F* are the distribution areas of $C_{12}A_7$ and the mass fractions of Na_2O doped in $C_{12}A_7$ at Points *E* and *F* are about 4.40% and 4.45%, respectively. So, the chemical formulae can be written as $0.92Na_2O \cdot 9.37CaO \cdot 7Al_2O_3$ and $0.94Na_2O \cdot 9.61CaO \cdot 7Al_2O_3$, respectively. The Na_2O content doped in $C_{12}A_7$ increases slightly from 4.33% to 4.45% when

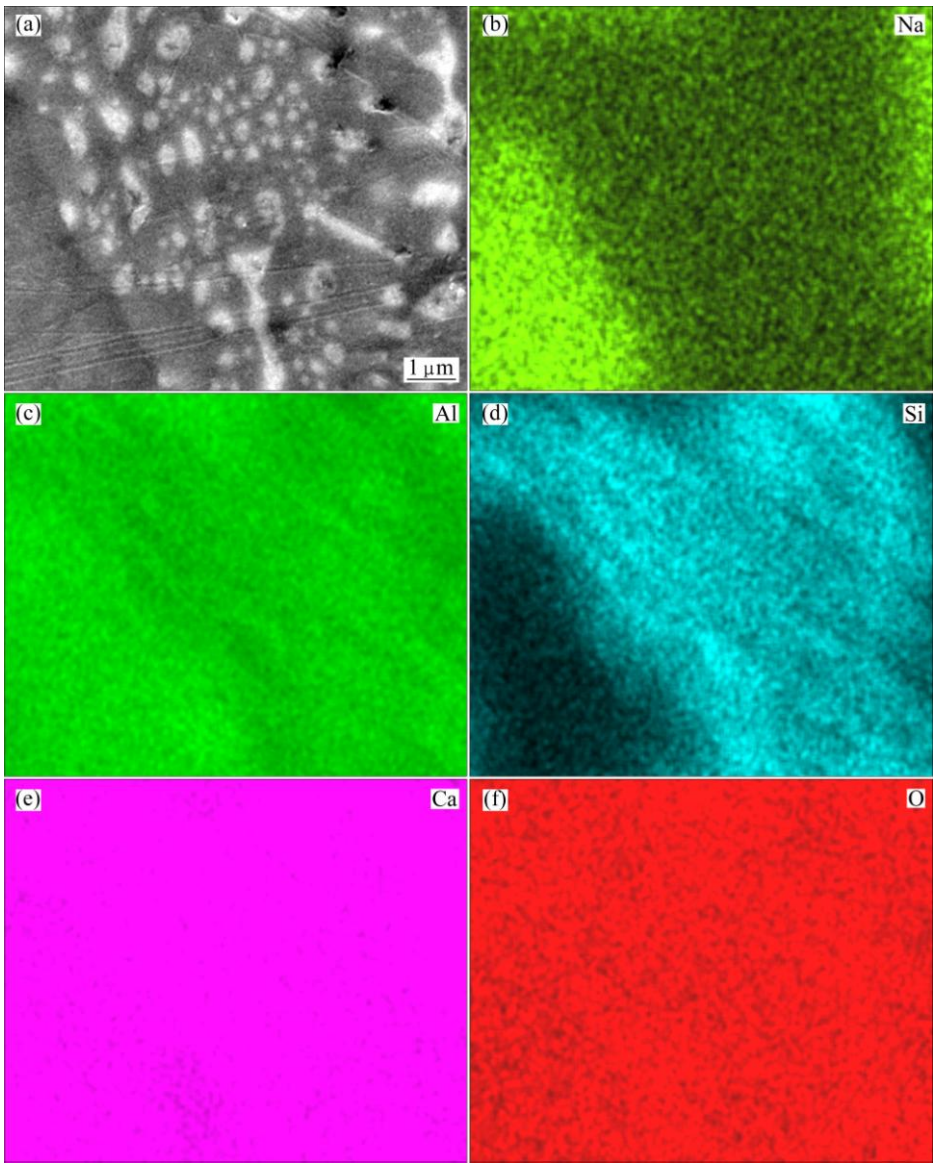

Fig. 5 SEM image (a) and scanning maps (b−f) of clinkers at N/A ratio of 0.04 and C/A ratio of 0.88

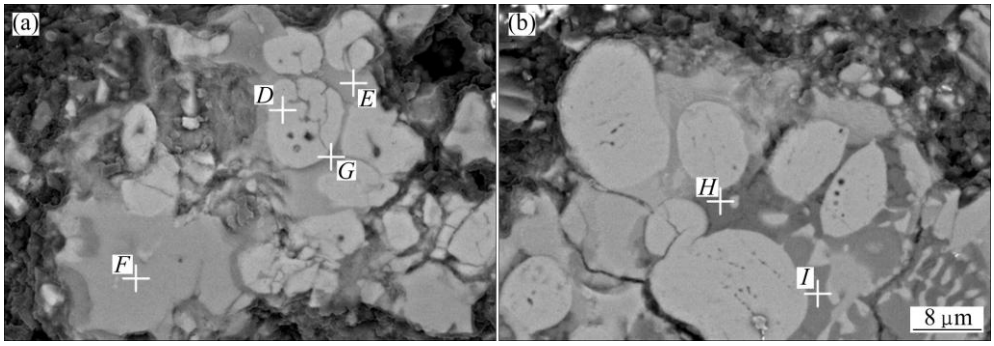

Fig. 6 BSE images of sintered clinkers at N/A ratio of 0.24 and C/A ratio of 0.87 in different zones: (a) Zones *D*, *E*, *F* and *G*; (b) Zones *H* and *I*

Table 4 Mole fractions of elements in clinkers determined by EDS

Point in Fig. 6	Mole fraction/%					Phase
	Na	Al	Si	Ca	O	
D	1.57	0.46	14.28	27.77	55.92	C_2S
E	2.93	22.34	1.38	17.71	55.65	$C_{12}A_7$
F	3.36	24.99	0.24	17.64	53.77	
G	0.48	13.14	−	25.16	61.23	CA
H	18.50	25.39	0.60	2.58	52.93	NA, $Na_4Ca_3(AlO_2)_{10}$
I	13.33	28.34	−	7.50	50.83	NA, $Na_4Ca_3(AlO_2)_{10}$

the N/A ratio is increased from 0.04 to 0.24. According to analysis results of Point *G*, the darker area at the edge of C_2S represents the region of CA. Trace amount of CA is formed when the N/A ratio of clinker is 0.24 and the content of Na_2O in the CA is about 1.43%. The results of element analysis of Points *H* and *I* confirm the existence of NA and $Na_4Ca_3(AlO_2)_{10}$. Moreover, NA and $Na_4Ca_3(AlO_2)_{10}$ are distributed in the same micro-regions.

The crystal system of CA is monoclinic and the space group is *P*21/*n*. The crystal system of $C_{12}A_7$ is cubic and the space group is *I*-43*d*. MIZUKAMI et al [16], SUSHKO et al [17] and HOSONO et al [18] reported that the $C_{12}A_7$ cell was constituted by sub-nanometer size cages, which was approximately 0.4 nm in diameter. Each $C_{12}A_7$ cell consisted of two molecules with twelve cages. Two free oxygen ions existed in the twelve cages. The free oxygen ion can be substituted by the hydroxide ion, chloride ion and fluoride ion without changing the crystal structure [19−23]. The radii of Ca^{2+} and Na^+ ions are 0.130 and 0.102 nm, respectively. The radii of OH^-, Cl^- and F^- ions are 0.137, 181 and 133 nm, respectively. They are all larger than the radius of Na^+ ion. Therefore, Na^+ ion may replace Ca^{2+} ion or the free oxygen ion of $C_{12}A_7$ without changing the crystal system and space group. The Ca^{2+} and O^{2-} ions of $C_{12}A_7$ cells are not distributed symmetrically, while those of CA cells are distributed symmetrically. Therefore, it is easier for polar molecules such as H_2O and Na_2O to penetrate the cells or react with the cells.

The crystallinities of phases are calculated through fitting the spectra using MDI Jade, which are shown in Fig. 7. Due to the doping of Na_2O in the crystal structures, the crystallinities of $C_{12}A_7$ and β-C_2S decrease with the rise of Na_2O content in clinkers. The crystallinity of $Na_4Ca_3(AlO_2)_{10}$ decreases with the increase of Na_2O content in clinkers. The reason may be the coexistence of NA and $Na_4Ca_3(AlO_2)_{10}$ and the unbalanced distribution of Na_2O between NA and $Na_4Ca_3(AlO_2)_{10}$. On the contrary, the crystallinity of CA increases slightly from 96.87% to 97.72% when the N/A ratio increases from 0 to 0.04. This is due to the fact that the ions in the defects of CA crystal structure have higher activity. Thus, the ions are easier to react with Na_2CO_3, which reduces the defects of CA grains. The increase of the crystallinity of CA also shows that it is difficult for Na_2O to insert the cells of CA. With the doping of Na_2O in clinkers, the crystallinity of γ-C_2S slightly decreases. Yet, the crystallinity of γ-C_2S rises slightly with the increase of Na_2O content in clinkers. However, the crystallinity of γ-C_2S in different clinkers is around 96.5%.

3.3 Simulation of Na_2O-doped $C_{12}A_7$ crystal

The analysis results of EDS show that Na_2O mainly

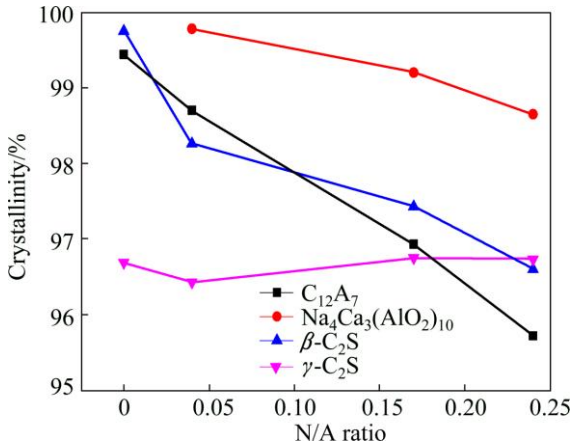

Fig. 7 Crystallinities of phases in clinkers at C/A ratio of about 0.85

coexists with $C_{12}A_7$ compared with other compounds. Material Studio was used to analyze the effect of Na_2O addition on the $C_{12}A_7$ cell. The setting values of the parameters during the optimization process of the crystal structures of $C_{12}A_7$ cells with or without Na_2O doping are the same to ensure the comparability of the results. As shown in Table 5, the convergence standards during the calculation process are also the same with each other. The crystal structure data illustrated in Table 6 are derived from the ICSD.

Table 5 Parameter settings for optimization of crystal structure of $C_{12}A_7$ cells during calculation

Status	Convergence/ (eV atom^{-1})	Displacement/ Å	Force/ (eV·Å^{-1})	Stress/ GPa
GGA-PBE	4.1393×10^{-5}	4.4963×10^{-4}	4.9123×10^{-3}	1.5383×10^{-2}

The primitive cell of $C_{12}A_7$, simulated by MS using the crystal structure data in Table 6, is shown in Fig. 8. The crystal structure of $C_{12}A_7$ has a high symmetry. Any Ca atom can be chosen to be replaced by Na atom. The results will be the same, since only one kind of Ca site exists in the structure. The cell, one Ca atom of which is substituted by one Na atom, is shown in Fig. 9.

Table 6 Crystal structure data and atomic coordinates of $C_{12}A_7$

Atom	Number	Valence	Site	x	y	z
Ca	1	+2	24d	0	0.250	0.140
Al	1	+3	16c	0.019	0.019	0.019
Al	2	+3	12d	−0.125	0	0.250
O	1	−2	48e	0.151	−0.037	0.057
O	2	−2	16c	−0.064	−0.064	−0.064
O	3	−2	24d	0	0.250	0.083

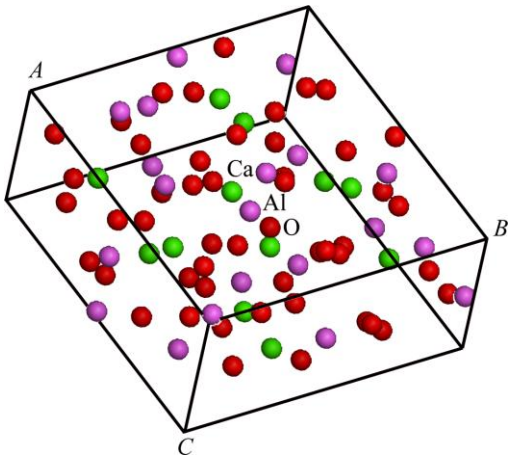

Fig. 8 Model of $C_{12}A_7$ unit cell

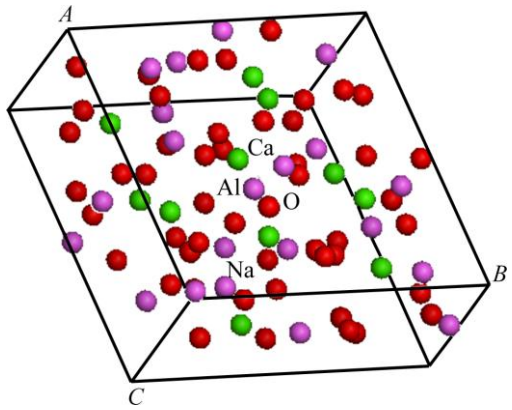

Fig. 9 Model of $C_{12}A_7$ unit cell when one Ca atom is replaced by one Na atom

The crystal structure of $C_{12}A_7$ mainly contains O—Al, O—Ca and O—O bonds. The bond length of O—Al is about 0.17 nm with the 3s and 3p orbital electrons of Al atom and the 2s, 2p orbital electrons of O atom forming the hybrid orbit. The bond length of O—Ca is about 0.24 nm with the 3s, 3p and 4s orbital electrons of Ca atom and the 2s, 2p orbital electrons of O atom forming the hybrid orbit. The bond population and length of $C_{12}A_7$ are presented in Table 7. The bond population is useful for evaluating the bonding character. A high value of the population of one chemical bond suggests that the bond is a covalent bond, whereas a low value suggests that the bond is an ionic bond [24,25]. As shown in Table 7, the population of the O—Al bond is much higher than that of the O—Ca bond, suggesting that the covalent character of the O—Al bond is stronger than that of the O—Ca bond. The O—O bonds are separated into two kinds, which show the covalent character and the ionic character, respectively. The bond of O—O with larger population is composed of the two free oxygen atoms in the cage-like structures. The computer cannot simulate the free oxygen atoms, so the free oxygen atoms may not form chemical bonds in the real materials.

Table 7 Bond population and length of $C_{12}A_7$

Chemical bond	Population	Length/nm
O—O	0.37	0.1276
O—Al	0.42	0.1785
	0.45	0.1762
	0.52	0.1749
O—Ca	0.06	0.2470
	0.09	0.2497
	0.10	0.2334
	0.13	0.2470
O—O	−0.06	0.2760
	−0.06	0.2761
	−0.04	0.2932
	−0.01	0.2934

Table 8 Bond population and length of $C_{12}A_7$ doped with one Na atom

Chemical bond	Population	Length /nm
O—O	0.37	0.1257
O—Al	0.42	0.1787
	0.45	0.1734
	0.52	0.1748
O—Na	0.03	0.2698
O—Ca	0.09	0.2345
	0.10	0.2459
	0.12	0.2471
O—O	−0.06	0.2768
	−0.06	0.2751
	−0.03	0.2934
	−0.02	0.2932

The bond population and length of $C_{12}A_7$ doped by one Na atom are shown in Table 8. The positions of the atoms in the crystals are changed in order to minimize the free energy of the cells and improve the stability of the cells during the simulation. The data in Table 8 suggest that the doping of Na atom does not significantly change the atomic distances and populations of O—Al and O—O bonds. Due to the replacement of Na atom, the species of O—Ca bond decrease from the original 4 to 3. As shown in Table 8, the population of O—Na bond is 0.03, which is lower than that of O—Ca bond. In addition, the O—Na bond has a larger atomic distance than O—Ca bond. Consequently, the covalency of the O—Na bond is weaker than that of the O—Ca bond.

The lattice parameter, the unit cell volume and the free energy of $C_{12}A_7$ unit cell and Na_2O-doped $C_{12}A_7$ cell are illustrated in Table 9. The doping of the Na atom has no significant effect on the lattice parameters and cell volumes. The free energy of the unit cell is increased because of the Na_2O addition. The free energy is the internal energy converted into other kind of energy during reactions. The simulation processes have been done under the hypothesis that the external environment conditions such as temperature and pressure are stable. Therefore, the free energy is the characteristic of the stability of the crystal structure. According to the principle of minimum energy, a lower free energy value corresponds to a higher activity. The increase of the free energy shows that the doping of Na atom can increase the chemical activity of $C_{12}A_7$, which benefits the leaching process of $C_{12}A_7$ in the sodium carbonate solution.

Table 9 Structural parameters of $C_{12}A_7$ and Na_2O-doped $C_{12}A_7$

Cell	Lattice parameter (a=b=c)/nm	Cell volume/nm^3	Free energy/eV
$C_{12}A_7$	1.2229	1.82883	−32139.20
Na_2O-doped $C_{12}A_7$	1.2025	1.73882	−31459.37

3.4 Leaching properties of sintered clinkers

CA, $C_{12}A_7$ and $Na_4Ca_3(AlO_2)_{10}$ can decompose in sodium carbonate solution. The processes are shown in Eqs. (3)−(5). Sodium hydroxide is also needed during the leaching process. The function of sodium hydroxide is to keep the stability of sodium aluminate in solution.

$$CaAl_2O_4+Na_2CO_3+4H_2O=CaCO_3\downarrow+2NaAl(OH)_4 \quad (3)$$

$$Ca_{12}Al_{14}O_{33}+12Na_2CO_3+33H_2O= 12CaCO_3\downarrow+14NaAl(OH)_4+10NaOH \quad (4)$$

$$Na_4Ca_3(AlO_2)_{10}+3Na_2CO_3+20H_2O= 3CaCO_3\downarrow+10NaAl(OH)_4 \quad (5)$$

The leaching results of clinkers are listed in Tables 10 and 11. As given in Table 10, the leaching efficiency of CA clinkers containing small quantity of $C_{12}A_7$ is 86.28%. The leaching efficiency increases to 96.79% when the N/A ratio increases from 0 to 0.33. The leaching efficiency of pure $Na_4Ca_3(AlO_2)_{10}$ is 97.15%, which suggests that $Na_4Ca_3(AlO_2)_{10}$ has a better leaching performance than CA. $Na_4Ca_3(AlO_2)_{10}$ is easier to react with carbon sodium solution. Thus, the molecular polarity of $Na_4Ca_3(AlO_2)_{10}$ is higher than that of CA. As given in Table 11, the leaching efficiency of Al_2O_3 of the clinkers increases from 34.81% to 88.17% as the N/A ratio increases from 0 to 0.24. The C/A ratio of raw materials can be decreased to 0.85 when mixed with Na_2O and the clinkers can also have proper leaching performance.

The leaching residues are almost washed to neutrality. The contents of Na_2O in residues, as shown in Tables 10 and 11, are almost the same. Moreover, the

Table 10 Leaching results of clinkers of Na_2O-doped $CaO-Al_2O_3$ system

C/A	N/A	Mass fraction of clinker/%		Mass fraction of residue/%			η_{AO}/%
		Al_2O_3	CaO	Al_2O_3	CaO	Na_2O	
1.0	0	62.57	36.48	11.65	49.49	0.86	86.28
1.0	0.33	54.45	31.63	2.87	51.99	0.97	96.79
0.60	0.40	63.59	20.95	4.36	50.45	0.90	97.15

Table 11 Leaching results of clinkers of Na_2O-doped $CaO-Al_2O_3-SiO_2$ system

N/A	Mass fraction of clinker/%		Mass fraction of residue/%			η_{AO}/%
	Al_2O_3	CaO	Al_2O_3	CaO	Na_2O	
0	30.62	50.24	19.43	48.90	0.75	34.81
0.04	30.20	49.98	18.06	50.60	0.61	40.93
0.17	28.57	49.19	10.40	54.94	0.70	67.41
0.24	29.44	48.05	4.22	58.20	0.66	88.17

Na_2O content in residues of clinkers without Na_2O is higher than that of clinkers doped with Na_2O. Thus, most of Na_2O in residues derives from the sodium carbonate or sodium hydroxide. Na_2O in compounds almost all dissolves in solution. It can be concluded that the improvement of leaching property of clinkers is attributed to the increase of $Na_4Ca_3(AlO_2)_{10}$ and $C_{12}A_7$ contents in clinkers and the improvement of the chemical activity of Na_2O-doped $C_{12}A_7$.

4 Conclusions

1) The phases containing Na_2O in clinkers of Na_2O-doped $CaO-Al_2O_3-SiO_2$ system mainly include $Na_4Ca_3(AlO_2)_{10}$ and $Na_2O\cdot Al_2O_3$. The rest of Na_2O is mainly doped in $C_{12}A_7$. It is easier for Na_2O to insert into the $C_{12}A_7$ cell than to insert into CA cell. The crystallinities of $Na_4Ca_3(AlO_2)_{10}$ and $C_{12}A_7$ decrease gradually with the increase of Na_2O content in clinkers while that of CA increases slightly.

2) The doping of Na_2O promotes the formation of $C_{12}A_7$ and $Na_4Ca_3(AlO_2)_{10}$ and prohibits the formation of C_2AS. The formation processes of $Na_4Ca_3(AlO_2)_{10}$ and $C_{12}A_7$ can be divided into two ways, which are the direct reactions among raw materials and the transformation of CA, respectively.

3) The covalency of O—Al is the strongest in the $C_{12}A_7$ cells. The covalency of the O—Na bond is weaker than that of the O—Ca bond, which results in the increase of the free energy of $C_{12}A_7$ crystal structure and the decrease of the structural stability of $C_{12}A_7$.

4) $C_{12}A_7$ and $Na_4Ca_3(AlO_2)_{10}$ have better leaching properties than CA. The leachability of clinker is increased because of the formation of $Na_4Ca_3(AlO_2)_{10}$, the increasing amount of $C_{12}A_7$ and the doping of Na_2O in $C_{12}A_7$ cells.

References

[1] YU Hai-yan, PAN Xiao-lin, WANG Bo, ZHANG Wu, SUN Hui-lan, BI Shi-wen. Effect of Na_2O on formation of calcium aluminates in $CaO-Al_2O_3-SiO_2$ system [J]. Transaction of Nonferrous Metals Society of China, 2012, 22(12): 3108−3112.

[2] WANG Bo, SUN Hui-lan, GUO Dong, ZHANG Xue-zheng. Effect of Na_2O on alumina leaching property and phase transformation of MgO-containing calcium aluminate slags [J]. Transaction of Nonferrous Metals Society of China, 2011, 21(12): 2752−2757.

[3] OSTROWSKI C, ZELAZNY J. Solid solutions of calcium aluminates C_3A, $C_{12}A_7$ and CA with sodium oxide [J]. Journal of Thermal Analysis and Calorimetry, 2004, 75(3): 867−885.

[4] TIAN Yong-pan, TU Gan-feng, PAN Xiao-lin, YU Hai-yan. Phase transformation and leaching performance of Na_2O-doping calcium aluminate compounds [J]. Journal of the Chemical Industry and Engineering Society of China, 2015, 66(4): 1151−1156. (in Chinese)

[5] FUKUDA K, INOUE S, YOSHIDA H. Substitution of sodium and silicon in tricalcium aluminate [J]. Journal of the American Ceramic Society, 2003, 86(1): 112−114.

[6] KANG E T, LEE S J, HANNON A C. Molecular dynamics simulations of calcium aluminate glasses [J]. Journal of Non-Crystalline Solid, 2006, 352(8): 725−736.

[7] EUGENIE V U, MICHAEL C W, NORBERT J K, AYDIN A G. Glass-forming ability in calcium aluminate-based systems [J]. Journal of the American Ceramic Society, 1993, 76(2): 449−453.

[8] SHAHRIAR I, JEKABS G, GUNNAR S, JESPER L, TOBIAS J, GIANLUIGI A B, CARMEN M A, HAKAN E. Phase formation of $CaAl_2O_4$ from $CaCO_3-Al_2O_3$ powder mixtures [J]. Journal of the European Ceramic Society, 2008, 28(4): 747−756.

[9] CHEN Guo-hua. Mechanical activation of calcium aluminate formation from $CaCO_3-Al_2O_3$ mixtures [J]. Journal of Alloys and Compounds, 2006, 416(1): 279−283.

[10] YI H C, GUIGNÉ J Y, MOORE J J, SCHOWENGERDT F D, ROBINSON L A, MANERBINO A R. Preparation of calcium aluminate matrix composites by combustion synthesis [J]. Journal of Materials Science, 2002, 37(21): 4537−4543.

[11] MARTIN R M. Electronic structure: Basic theory and practical methods [M]. London: Cambridge University Press, 2004: 566−569.

[12] BRIK M G, AVRAM N M, GRUIA A S. Calculation of the spectral, structural, and electronic properties of $NaCrSi_2O_6$ and $LiCrSi_2O_6$

crystals [J]. Optical Materials, 2013, 35(10): 1772−1775.

[13] WU Y Q, YOU J L, JIANG G C. Molecular dynamics study of the structure of calcium aluminate melts [J]. Journal of Inorganic Materials, 2003, 18(3): 619−626.

[14] PAN Xiao-lin, YU Hai-yan, TIAN Yong-pan, SU Hang, TU Gan-feng, BI Shi-wen. Computer simulation of crystal stability of $12CaO\cdot7Al_2O_3$ with calcium vacancy [J]. The Chinese Journal of Nonferrous Metals, 2014, 24(11): 2914−2920. (in Chinese)

[15] GREENE K T, BOGUE R H. Phase equilibrium relations in a portion of the system $Na_2O-CaO-Al_2O_3-SiO_2$ [J]. Journal of Research of the National Bureau of Standards (U.S.), 1946, 36(2) 185−207.

[16] MIZUKAMI F, CHATTERJEE A, NISHIOKA M. A periodic first principle study to design microporous crystal $12MO\cdot7A1_2O_3$ for selective and active O-radicals encaging [J]. Chemical Physics Letters 2004, 390(4): 335−339.

[17] SUSHKO P V, SHLUGER A L, KATSURO H, MASAHIRO H, HIDEO H. Localisation assisted by the lattice relaxation and the optical absorption of extra-framework electrons in $12CaO\cdot7A1_2O_3$ [J]. Materials Science and Engineering C, 2005, 25(5): 722−726.

[18] HOSONO H, KIM S W, MIYAKAWA M, MATSUISHI S, KAMIYA T. Thin film and bulk fabrication of room-temperature-stable electride $C_{12}A_7$:e utilizing reduced amorphous $12CaO\cdot7A1_2O_3(C_{12}A_7)$ [J]. Journal of Non-Crystalline Solids, 2008, 354(19): 2772−2776.

[19] PALACIOS L, ÁNGELES G, TORRE D L, BRUQUE S, JOSE L, SANTIAGO G G, SHEPTYAKOV D, MIGUEL A G. Crystal structures and in-situ formation study of mayenite electrides [J]. Inorganic Chemistry, 2007, 46(10): 4167−4176.

[20] NISHIOA Y, NOMURAB K, YANAGIA H, KAMIYA T, HIRANO M, HOSONO H. Short-channel nanowire transistor using a nanoporous crystal semiconductor $12CaO\cdot7Al_2O_3$ [J]. Materials Science and Engineering B, 2010, 173(1): 37−40.

[21] MIYAKAWA M, TODA Y, HAYASHI K, HIRANO M, KAMIYA T, MATSUNAMI N, HOSONO H. Formation of inorganic electride thin films via site-selective extrusion by energetic inert gas ions [J]. Journal of Applied Physics, 2005, 97(2): 023510.

[22] KIM S W, SHIMOYAMA T, HOSONO H. Solvated electrons in high-temperature melts and glasses of the room-temperature stable electride $[Ca_{24}Al_{28}O_{64}]^{4+}\cdot4e^-$ applied [J]. Science, 2011, 333: 71−74.

[23] HAYASHI K, MATSUISHI S, KAMIYA T, HIRANO M, HOSONO H. Light-induced conversion of an insulating refractory oxide into a persistent electronic conductor [J]. Nature, 2002, 419: 462−465.

[24] MULLIKEN R S. Electronic population analysis on LCAO–MO molecular wave functions: I [J]. Journal of Chemical Physics, 1955, 23: 1833−1840.

[25] KHADRAOUI Z, BOUZIDI C, HORCHANI-NAIFER K, FERID M. Crystal structure, energy band and optical properties of dysprosium monophosphate $DyPO_4$ [J]. Journal of Alloys and Compounds, 2014, 617: 281−286.

Na_2O 掺杂铝酸钙化合物的形成机理与晶体模拟

田勇攀，潘晓林，于海燕，涂赣峰

东北大学 冶金学院，沈阳 110819

摘　要：采用分析纯试剂 $CaCO_3$、Al_2O_3、SiO_2 和 Na_2CO_3 合成 Na_2O 掺杂铝酸钙熟料，研究 Na_2O 掺杂对铝酸钙化合物形成机理及 $12CaO\cdot7Al_2O_3(C_{12}A_7)$晶体结构的影响。结果表明：当熟料中 Na_2O 含量低于 4.26%(质量分数)时，含 Na_2O 物相主要为 $2Na_2O\cdot3CaO\cdot5Al_2O_3$ 和 $Na_2O\cdot Al_2O_3$；其余 Na_2O 主要掺杂在 $12CaO\cdot7Al_2O_3$ 内，并且使其结晶度降低。$2Na_2O\cdot3CaO\cdot5Al_2O_3$ 的结晶度也随着熟料中 Na_2O 含量升高而降低。$2Na_2O\cdot3CaO\cdot5Al_2O_3$ 和 $12CaO\cdot7Al_2O_3$ 的生成途径有两种方式：一是由初始反应物的直接反应生成，二是由反应中间产物 $CaO\cdot Al_2O_3$ 的进一步转化反应生成。晶体结构模拟结果表明，在 Na_2O 掺杂的 $12CaO\cdot7Al_2O_3$ 晶格内，其 O—Na 键的共价性弱于 O—Ca 键和 O—Al 键的共价性，使 $12CaO\cdot7Al_2O_3$ 晶胞自由能升高，化学活性提高。当熟料中 Na_2O 含量由 0 增加至 4.26%时，Al_2O_3 的浸出率由 34.81%增大至 88.17%。

关键词：铝酸钙；Na_2O 掺杂；形成机理；晶体结构；烧结；计算机模拟

(Edited by Wei-ping CHEN)